

## SUPPORTING INFORMATION

### Solvent-Induced Membrane Stress in Biofuel Production: Molecular Insights from Small-Angle Scattering and All-Atom Molecular Dynamics Simulations

**Micholas Dean Smith, Sai Venkatesh Pingali, James Elkins, Dima Bolmatov, Robert Standaert, Jonathan Nickels, Volker Urban, John Katsaras, Brian Davison, Jeremy C. Smith, Loukas Petridis**

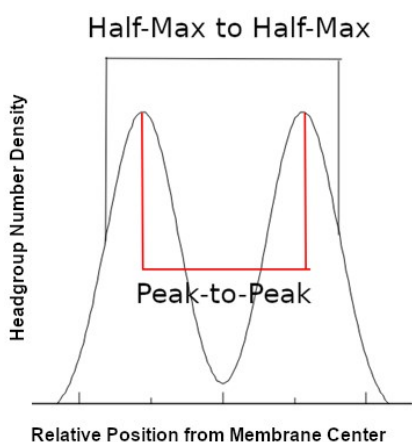
The results presented in Figure 2 were obtained by fitting (using SASView) the experimental scattering intensity (Figure S1 and S2),  $I(Q)$ , using the following model:

$$I(Q) = \left[ \int P(R_C, Q) f(R_C) dR_C \right] * S(Q),$$

where  $P(R_C, Q)$  and  $S(Q)$  are the form and structure factors, respectively. The form factor for a spherical core-multi-shell model with a polydisperse spherical core is given by the expression:

$$P(R_C, Q) = \frac{Scale}{V_{S3}} \left[ 3V_C(\rho_C - \rho_{S1}) \frac{[\sin(qR_C) - qR_C \cos(qR_C)]}{(qR_C)^3} + \sum_{i=1}^2 3V_{Si}(\rho_{Si} - \rho_{S(i+1)}) \frac{[\sin(qR_{Si}) - qR_{Si} \cos(qR_{Si})]}{(qR_{Si})^3} \right] + Bkg,$$

where *scale* is a scale factor,  $V_C$  is the volume of the core,  $V_{S1}$ ,  $V_{S2}$ , and  $V_{S3}$  are the volumes of the inner-most, middle, and outermost shells, respectively;  $R_C$  is the radius of the core and  $R_{S1}$ ,  $R_{S2}$ , and  $R_{S3}$  are the radii of the inner-most, middle, and outermost shells, respectively;  $\rho_C$  is the scattering length density of the core,  $\rho_{S1}$ ,  $\rho_{S2}$  and,  $\rho_{S3}$  are the scattering length density of the inner-most, middle, and outermost shells, respectively, and  $\rho_{solv}$  is the scattering length density of the solvent; and *Bkg* is the background intensity level. The spherical core's radial polydispersity was modeled as having a Gaussian distribution. The hard-sphere structure factor, as implemented in SASView, is for monodisperse spherical particles interacting through hard-sphere (excluded volume) interactions. The Percus-Yevick closure is used for these calculations, and the interparticle potential is:



$$U(r) = \begin{cases} \infty, & r < 2R \\ 0, & r \geq 2R \end{cases}$$

where  $r$  is the distance from the center of a sphere with radius  $R$ .

**Illustration S1.** Schematic description of membrane thickness measurements. Peak-to-Peak distances correspond to a distance depicted by the horizontal red-line, while Half-Max to Half-Max corresponds to the black horizontal line. Half-Max corresponds to x-coordinate location the corresponds with a y-value that is half the maximum height of the distribution. This schematic is shown to provide a sense of how distances between the leaflets were calculated for use in the derivation of the membrane thicknesses presented in the main text and should only be use for illustrative purposes. Further, it should be noted that the instantaneous phosphate distributions will not be smooth for every frame of the MD trajectories, but does take the same approximate shape as what is shown above.

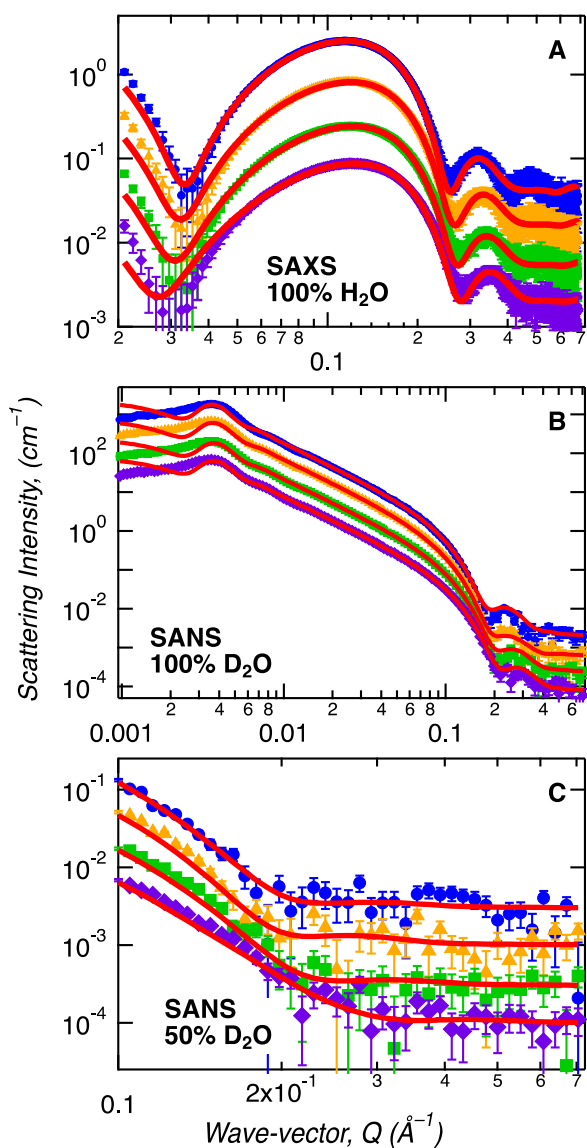


**Figure S1.** Scattering intensity profiles of POPE/POPG (70:30) unilamellar lipid vesicles (ULVs) measured as a function of butanol concentrations of 0%, 1%, 2% and 3% by: (A) SAXS in 100% H<sub>2</sub>O; (B) by SANS in 100% D<sub>2</sub>O; and (C) by SANS in 50% D<sub>2</sub>O. The solid red lines are fits to the data using the spherical core-multi-shell model with a polydisperse spherical core and hard sphere interactions. Butanol concentrations are 0% (blue dots), 1% (orange filled up-triangles), 2% (green filled squares), and 3% (purple filled diamonds). Not shown in this plot, but used for analysis of the data, was a SANS measurement of ULVs in 70% D<sub>2</sub>O.

Small-angle X-ray/neutron scattering (SAXS/SANS) were combined synergistically to elucidate the POPE:POPG (70:30) lipid bilayer structure and changes in the structure when subjected to a increasing concentrations of butanol (0-3 wt%) and THF (0-6 wt%) solvents (Figures S1 and S2). Each scattering technique is only sensitive to parts of this complex system- X-rays are sensitive to the head groups and consequently the overall bilayer thickness, whereas neutron scattering is more sensitive to the tail groups. Furthermore, by leveraging the large difference in neutron sensitivity between hydrogen and deuterium atoms, the relative strengths of the scattering of the head and tail groups relative to solvent is varied by studying the systems in at least 3 different D<sub>2</sub>O:H<sub>2</sub>O solvent ratios. Combined, a global picture of the bilayer structure including the internal head and tail group regions of the lipid bilayer is thus obtained. For each sample condition, we collected four different contrast data sets: (A) SAXS in 100% H<sub>2</sub>O; (B) SANS in 100% D<sub>2</sub>O; (C) SANS in 50% D<sub>2</sub>O; and (D) SANS in 70% D<sub>2</sub>O (not shown in Figures S1 and S2). These SANS scattering profiles represent solvent filled unilamellar lipid vesicles (ULVs) and are fitted by a spherical core-multi-shell model with a polydisperse spherical core and hard sphere interactions. The core of the ULV is filled with bulk solvent. The lipid bilayer arrangement in the ULV spherical shell is modeled to contain three shells. The lipid head groups in the outer and inner leaflet form two of these shells. The central shell contains the lipid tail groups from both the leaflets as a single shell. The results from this integrative analysis are summarized in Figure 2.

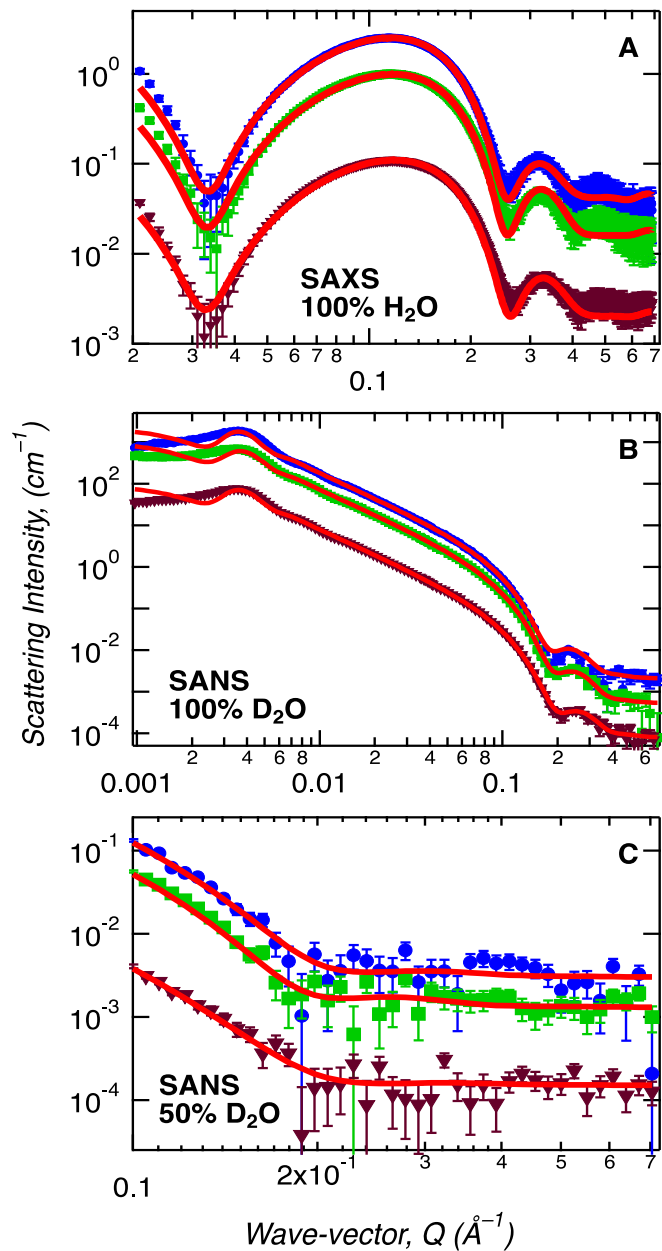


**Figure S2.** Scattering profiles of POPE/POPG (70:30) unilamellar vesicles (ULVs) measured as a function of tetrahydrofuran (THF) concentration concentrations of 0, 2 and 6 wt% by: (A) SAXS in 100% H<sub>2</sub>O; (B) by SANS in 100% D<sub>2</sub>O; and (C) by SANS in 50% D<sub>2</sub>O. The solid red lines are fits to the data using the spherical core-multi-shell model with a polydisperse spherical core and hard sphere interactions. THF concentrations are 0% (blue dots), 2% (green filled squares), and 6% (brown filled down-triangles). Not shown in this plot, but used for analysis of the data, was a SANS measurement of ULVs in 70% D<sub>2</sub>O.

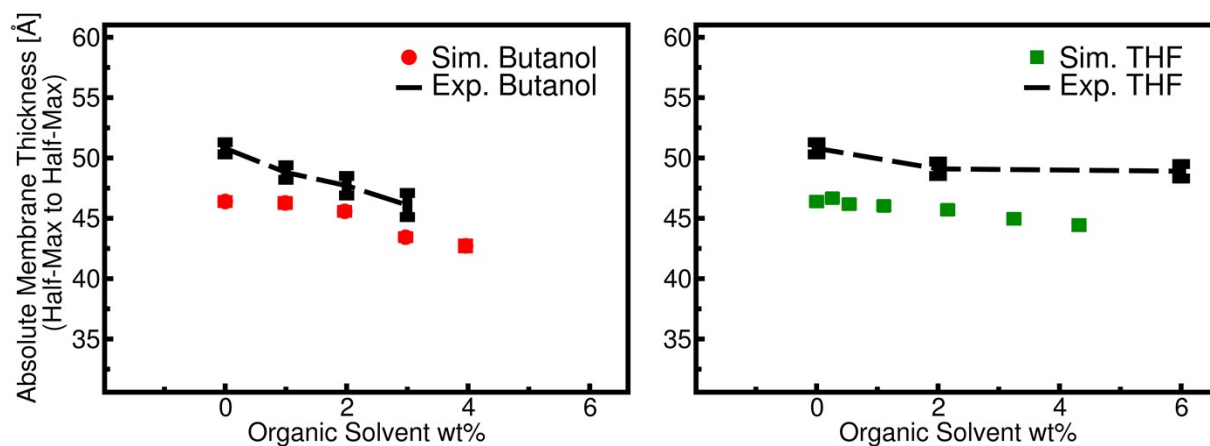


**Figure S3.** Direct comparison of absolute thicknesses between simulation (half-max to half-max) and experiment. Error bars are standard errors.

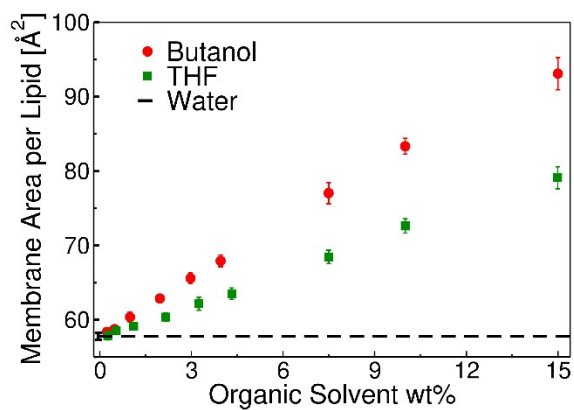


**Figure S4.** Area per lipid from MD simulation. Error bars are standard-error of the mean. The area per lipid was obtained assuming no acyl chain interdigitation and was considered to vary inversely with the bilayer thickness.

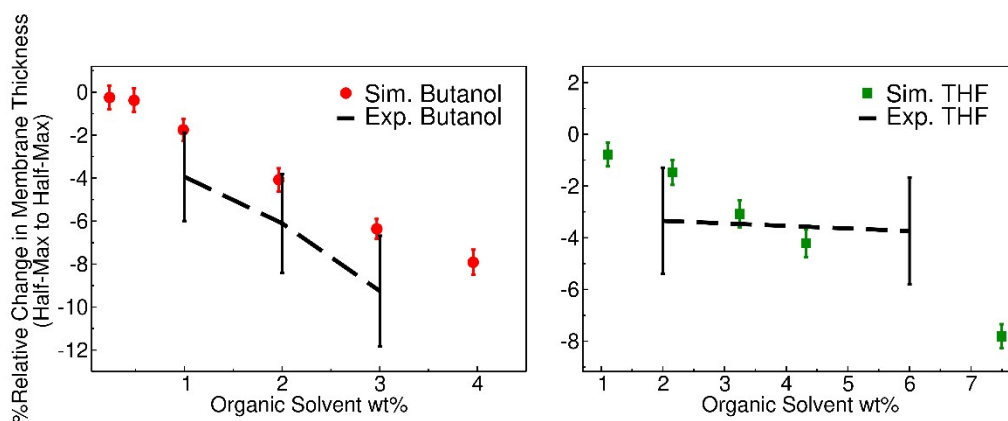


**Figure S5.** Comparison of the experiment and simulation (Half-Max-to-Half-Max) determined fractional relative change in the overall membrane thickness as a function of (A) THF and (B) butanol solvents in the POPE:POPG (3:1) lipid bilayer system.

Figure S6:

Figure S6 provides a view of the density profiles of the acyl tails from the last 25ns of the simulations. The narrowing of profiles and loss of distinct peaks correspond with the disruption of tail order (also characterized in Figure 5 of the main text) and the thinning of the membrane under the THF and butanol stresses.

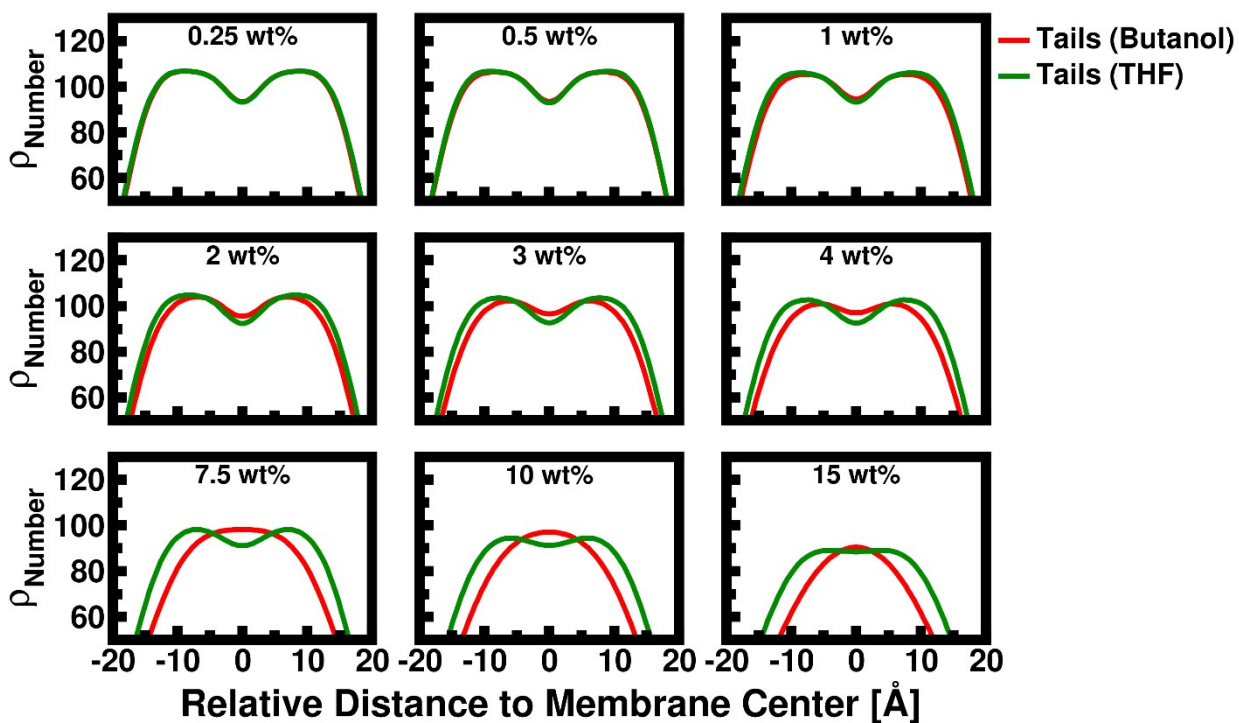


**Figure S6.** Computationally derived tail-density profiles averaged over all tail atoms and by joining the last 25ns from each independent simulation and calculating the density profile using the gmx density tool.

Figure S7:

Lateral diffusion constants (Figure 7) were computed, as noted in the main text, via fitting a line to the lateral mean-squared displacement curves shown below. If the mean-squared displacements contain any non-linearity, strictly speaking any diffusion constant obtained is an approximation. Here we note that although the curves are non-linear, this non-linearity is weak which suggests that the linear fitting approach provides reasonable diffusion constant estimates. Furthermore the trends with concentration over the mean-squared displacement curves in Figure S7 are also consistent with increased lipid mobility and membrane fluidization.

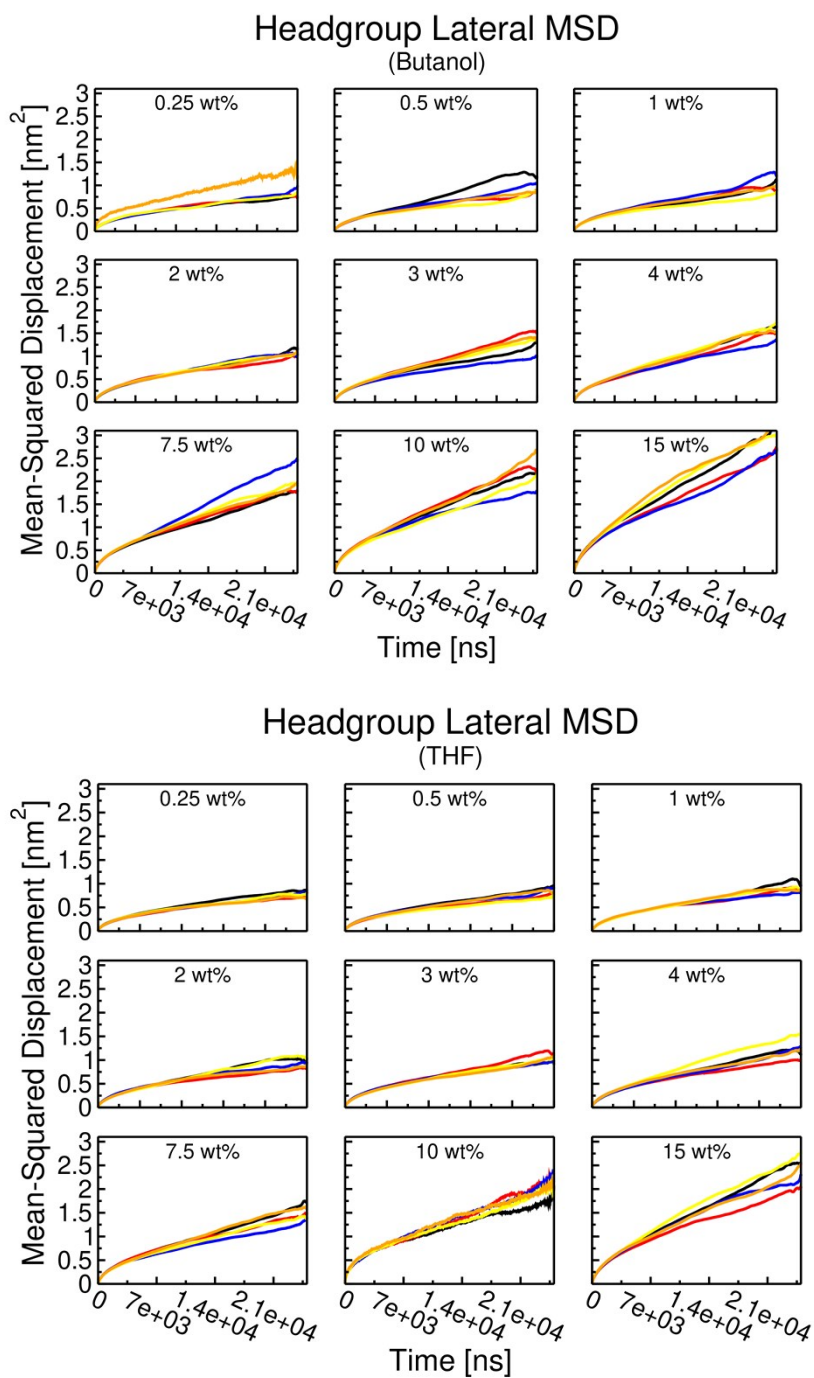


**Figure S7.** Mean-squared lateral displacement of lipid-head groups over the last 25ns of each simulation trajectory. Note the weakly non-linear trends.

**Table S1.** Parameters obtained from fits to different contrast small-angle scattering data of a pure POPE: POPG (3:1) bilayer system using the spherical core-multi-shell with radial polydispersity and hard-sphere interactions.

	SAXS	SANS		
	100% H <sub>2</sub> O	100% D <sub>2</sub> O	70% D <sub>2</sub> O	50% D <sub>2</sub> O
Scale (cm <sup>-1</sup> )	8.57 ± 0.06	0.427 ± 0.008	0.45 ± 0.05	0.45 ± 0.05
Background (cm <sup>-1</sup> )	0.04	0.002	0.002	0.003
$\rho_{\text{solvent}} \& \rho_{\text{core}}$ (x10 <sup>-6</sup> Å <sup>-2</sup> )	9.44	6.34	4.28	2.91
$R_{\text{core}}$ (Å)	846	846 ± 1	846	846
$\rho_{\text{head}}$ (x10 <sup>-6</sup> Å <sup>-2</sup> )	11.1 ± 0.7	5.73 ± 0.09	3.50 ± 0.07	2.52 ± 0.07
$d_{\text{head}}$ (Å)	13.7 ± 0.5	7.3	9.8	10.9
$\rho_{\text{tail}}$ (x10 <sup>-6</sup> Å <sup>-2</sup> )	7.85	-0.29	-0.29	-0.29
$d_{\text{tail}}$ (Å)	23.3 ± 0.7	36.3 ± 0.4	31.1 ± 0.7	28.9 ± 0.9
Volume Fraction, $\phi$		0.398 ± 0.001	0.398	0.398
Polydispersity $R_{\text{core}}$	0.377	0.377 ± 0.001	0.377	0.377
$d_{\text{tot}}$ (Å)	50.8 ± 0.5			

**Table S2.** Parameters obtained from fits to different contrast small-angle scattering data of a POPE: POPG (3:1) bilayer system with 1.0 wt% butanol using the spherical core-multi-shell with radial polydispersity and hard-sphere interactions

	SAXS	SANS		
	100% H <sub>2</sub> O	100% D <sub>2</sub> O	70% D <sub>2</sub> O	50% D <sub>2</sub> O
Scale (cm <sup>-1</sup> )	8.01 ± 0.06	0.45 ± 0.01	0.49 ± 0.04	0.42 ± 0.06
Background (cm <sup>-1</sup> )	0.04	0.0015	0.003	0.0025
$\rho_{\text{solvent}} \& \rho_{\text{core}}$ (x10 <sup>-6</sup> Å <sup>-2</sup> )	9.42	6.34	4.30	2.94
$R_{\text{core}}$ (Å)	824	824 ± 1	824	824
$\rho_{\text{head}}$ (x10 <sup>-6</sup> Å <sup>-2</sup> )	11.0 ± 0.7	5.1 ± 0.1	3.40 ± 0.07	2.42 ± 0.07
$d_{\text{head}}$ (Å)	13.0 ± 0.5	8.1	9.8	9.9
$\rho_{\text{tail}}$ (x10 <sup>-6</sup> Å <sup>-2</sup> )	7.85	-0.29	-0.29	-0.29
$d_{\text{tail}}$ (Å)	22.8 ± 0.6	32.5 ± 0.5	29 ± 1	29 ± 1
Volume Fraction, $\phi$		0.370 ± 0.001	0.370	0.370
Polydispersity $R_{\text{core}}$	0.383	0.383 ± 0.001	0.383	0.383
$d_{\text{tot}}$ (Å)	48.7 ± 0.6			



**Table S3.** Parameters obtained from fits to different contrast small-angle scattering data of a POPE: POPG (3:1) bilayer system with 2.0 wt% butanol using the spherical core-multi-shell with radial polydispersity and hard-sphere interactions

	SAXS		SANS	
	100% H <sub>2</sub> O	100% D <sub>2</sub> O	70% D <sub>2</sub> O	50% D <sub>2</sub> O
Scale (cm <sup>-1</sup> )	7.81 ± 0.05	0.469 ± 0.008	0.48 ± 0.05	0.45 ± 0.05
Background (cm <sup>-1</sup> )	0.04	0.00175	0.002	0.00225
$\rho_{\text{solvent}}$ & $\rho_{\text{core}}$ (x10 <sup>-6</sup> Å <sup>-2</sup> )	9.41	6.34	4.32	2.97
$R_{\text{core}}$ (Å)	817	817 ± 1	817	817
$\rho_{\text{head}}$ (x10 <sup>-6</sup> Å <sup>-2</sup> )	11.0 ± 0.7	5.54 ± 0.11	3.79 ± 0.08	2.55 ± 0.07
$d_{\text{head}}$ (Å)	12.7 ± 0.4	7.7	9.1	10.3
$\rho_{\text{tail}}$ (x10 <sup>-6</sup> Å <sup>-2</sup> )	7.85	-0.29	-0.29	-0.29
$d_{\text{tail}}$ (Å)	22.3 ± 0.7	32.2 ± 0.4	29.0 ± 0.8	27.0 ± 1.0
Volume Fraction, $\phi$		0.369 ± 0.001	0.369	0.369
Polydispersity $R_{\text{core}}$	0.356	0.356 ± 0.001	0.356	0.356
$d_{\text{tot}}$ (Å)	47.7 ± 0.8			

**Table S4** Parameters obtained from fits to different contrast small-angle scattering data of a POPE: POPG (3:1) bilayer system with 3.0 wt% butanol using the spherical core-multi-shell with radial polydispersity and hard-sphere interactions.

	SAXS		SANS	
	100% H <sub>2</sub> O	100% D <sub>2</sub> O	70% D <sub>2</sub> O	50% D <sub>2</sub> O
Scale (cm <sup>-1</sup> )	8.64 ± 0.08	0.486 ± 0.008	0.51 ± 0.05	0.60 ± 0.05
Background (cm <sup>-1</sup> )	0.04	0.0015	0.002	0.002
$\rho_{\text{solvent}}$ & $\rho_{\text{core}}$ (x10 <sup>-6</sup> Å <sup>-2</sup> )	9.39	6.35	4.34	3.00
$R_{\text{core}}$ (Å)	832	832 ± 1	832	832
$\rho_{\text{head}}$ (x10 <sup>-6</sup> Å <sup>-2</sup> )	10.9 ± 0.7	5.74 ± 0.09	3.75 ± 0.07	2.45 ± 0.09
$d_{\text{head}}$ (Å)	12.1 ± 0.5	7.8	9.8	13.3
$\rho_{\text{tail}}$ (x10 <sup>-6</sup> Å <sup>-2</sup> )	7.85	-0.29	-0.29	-0.29
$d_{\text{tail}}$ (Å)	22.0 ± 0.7	30.4 ± 0.4	27.0 ± 0.7	19.0 ± 1.0
Volume Fraction, $\phi$		0.376 ± 0.001	0.376	0.376
Polydispersity $R_{\text{core}}$	0.330	0.330 ± 0.001	0.330	0.330
$d_{\text{tot}}$ (Å)	46.1 ± 1.0			

**Table S5.** Parameters obtained from fits to different contrast small-angle scattering data of a POPE: POPG (3:1) bilayer system with 2.0 wt% tetrahydrofuran using the spherical core-multi-shell with radial polydispersity and hard-sphere interactions.

	SAXS		SANS	
	100% H <sub>2</sub> O	100% D <sub>2</sub> O	70% D <sub>2</sub> O	50% D <sub>2</sub> O
Scale (cm <sup>-1</sup> )	8.02 ± 0.07	0.504 ± 0.008	0.48 ± 0.05	0.47 ± 0.05
Background (cm <sup>-1</sup> )	0.04	0.00125	0.00225	0.00325
$\rho_{\text{solvent}} \& \rho_{\text{core}}$ (x10 <sup>-6</sup> Å <sup>-2</sup> )	9.42	6.34	4.32	2.97
$R_{\text{core}}$ (Å)	794	749 ± 1	749	749
$\rho_{\text{head}}$ (x10 <sup>-6</sup> Å <sup>-2</sup> )	11.3 ± 0.7	5.34 ± 0.13	3.35 ± 0.09	2.5702 ± 0.09
$d_{\text{head}}$ (Å)	12.4 ± 0.5	7.6	8.8	8.7
$\rho_{\text{tail}}$ (x10 <sup>-6</sup> Å <sup>-2</sup> )	7.85	-0.29	-0.29	-0.29
$d_{\text{tail}}$ (Å)	24.3 ± 0.7	34.1 ± 0.4	32.0 ± 1.0	32.0 ± 1.0
Volume Fraction, $\phi$		0.343 ± 0.001	0.343	0.343
Polydispersity $R_{\text{core}}$	0.399	0.399 ± 0.001	0.399	0.399
$d_{\text{tot}}$ (Å)	49.2 ± 0.6			

**Table S6.** Parameters obtained from fits to different contrast small-angle scattering data of a POPE: POPG (3:1) bilayer system with 6.0 wt% tetrahydrofuran using the spherical core-multi-shell with radial polydispersity and hard-sphere interactions.

	SAXS		SANS	
	100% H <sub>2</sub> O	100% D <sub>2</sub> O	70% D <sub>2</sub> O	50% D <sub>2</sub> O
Scale (cm <sup>-1</sup> )	8.34 ± 0.06	0.462 ± 0.008	0.50 ± 0.05	0.26 ± 0.05
Background (cm <sup>-1</sup> )	0.04	0.0015	0.0015	0.003
$\rho_{\text{solvent}} \& \rho_{\text{core}}$ (x10 <sup>-6</sup> Å <sup>-2</sup> )	9.38	6.34	4.41	3.11
$R_{\text{core}}$ (Å)	839	839 ± 1	839	839
$\rho_{\text{head}}$ (x10 <sup>-6</sup> Å <sup>-2</sup> )	11.1 ± 0.7	5.62 ± 0.10	3.55 ± 0.07	2.56 ± 0.07
$d_{\text{head}}$ (Å)	12.7 ± 0.5	8.1	9.8	11.0
$\rho_{\text{tail}}$ (x10 <sup>-6</sup> Å <sup>-2</sup> )	7.85	-0.29	-0.29	-0.29
$d_{\text{tail}}$ (Å)	23.5 ± 0.7	32.8 ± 0.4	29.4 ± 1.0	26.9 ± 2.0
Volume Fraction, $\phi$		0.368 ± 0.001	0.368	0.368
Polydispersity $R_{\text{core}}$	0.350	0.350 ± 0.001	0.350	0.350
$d_{\text{tot}}$ (Å)	48.9 ± 0.6			